Spatial trapping of short pulses in Ti-indiffused $LiNbO_3$ waveguides

Paul Pioger, Vincent Couderc, Laurent Lefort, and Alain Barthelemy

Faculte des Sciences, Institut de Recherches en Communications Optiques et Microondes, 123 Avenue A. Thomas, 87060 Limoges, France

Fabio Baronio and Costantino De Angelis

Dipartimento di Electtronica per l'Automazione, Istituto Nazionale per la Fisica della Materia, Università di Brescia, via Branze 38, 25123 Brescia, Italy

Yoohong Min, Victor Quiring, and Wolfgang Sohler

Angewandte Physik, Universität-GH Paderborn, 33095 Paderborn, Germany

Received July 2, 2002

We show numerically and experimentally that spatial trapping can be induced in quadratic media even if the pump pulse's duration is shorter than the group-delay mismatch between fundamental wave and second-harmonic components. The influence of phase mismatch and pulse power on the trapping effect is discussed. Spatial, temporal, and spectral behaviors that accompany self-trapped propagation are highlighted. © 2002 Optical Society of America

OCIS codes: 190.0190, 190.4420, 070.4340, 060.5530.

Cascaded $\chi^{(2)}$:$\chi^{(2)}$ parametric interactions of high-intensity light beams in materials with quadratic nonlinearities offer a rich variety of phenomena.[1] In particular, they can yield strong nonlinear refraction effects at relatively low power levels. Thus second-order cascading processes have gained relevance similar to that of their third-order counterparts for use in switching devices that rely on large optically induced nonlinear phase changes. Even though this subject has been investigated since the early 1970s,[2] only recently has it been revisited and applied to all-optical signal processing with the purpose of overcoming the limits of $\chi^{(3)}$ materials.[3–6]

We refer to electromagnetic nonlinear type I interaction of a fundamental wave [(FF) at 1548 nm] and a second-harmonic wave [(SH) at 774 nm]. We investigate the possibility of exciting spatially trapped beams in periodically poled Ti-indiffused lithium niobate slab waveguides with pulsed excitation, with only the FF at the input. The trapping is defined as the equivalence of the output and the input beam sizes. Because of the group-velocity mismatch between the FF and the SH, for short-pulse laser excitation it was predicted that one might expect serious difficulties in the generation of a spatially self-trapped beam near phase matching and that spatial soliton trapping would be possible only for a large mismatch.[7] The minimum pulse width is of paramount relevance, as it will give the limit of the processing speed of the envisaged all-optical devices. In this Letter we report experimental results, supported by numerical simulations, for one-dimensional self-trapped propagation with a pulsed excitation, at the FF only, that is almost five times shorter than the time walk-off between FF and SH.

The experiments were performed with an all-fiber laser system as the source of 4-ps pulses (FHWM) at 1548 nm (fundamental wavelength). The 58-mm-long Ti-indiffused lithium niobate Z-cut planar waveguide has constant ferroelectric domain periodicity of 16.92 μm. The sample was inserted into a temperature-stabilized oven to permit operation at elevated temperatures (120–160 °C); in this way, photorefractive effects (optical damage) could be minimized. Moreover, temperature tuning of the phase-matching conditions became possible. The laser beam was shaped in a highly elliptical spot, nearly Gaussian in profile, with FWHM $w_{0x} = 76$ μm along the waveguide plane and FWHM $w_{0y} = 3.9$ μm along the perpendicular direction. The spatial beam profiles were recorded by scanning a magnified image of the pattern with a photodiode. Temporal characterizations were monitored by a noncollinear SH-generation autocorrelator.

In a slab waveguide the electric fields E_1 and E_2, at ω_0 and $2\omega_0$, respectively, propagating in the z direction can be written as

$$E_1(x,y,z,t) = \tfrac{1}{2}\,(W(y)w(x,z,t) \times \exp\{-j[\beta(\omega_0)z + \omega_0 t]\} + \text{c.c.})\,,$$

$$E_2(x,y,z,t) = \tfrac{1}{2}\,(V(y)v(x,z,t) \times \exp\{-j[\beta(2\omega_0)z + 2\omega_0 t]\} + \text{c.c.})\,,$$

where $W(y)$ and $V(y)$ are the mode profiles at the FF and the SH in the guided dimension and $w(x, z, t)$ and $v(x, z, t)$ are the slowly varying envelopes. After averaging over the quasi-phase-matched periods, at the lowest order $w(x, z, t)$ and $v(x, z, t)$ obey the nonlinear coupled equations[1]

0146-9592/02/242182-03$15.00/0

$$j\frac{\partial w}{\partial z} - j\beta_{\omega_0}{}'\frac{\partial w}{\partial t} - \frac{\beta_{\omega_0}{}''}{2}\frac{\partial^2 w}{\partial t^2} + \frac{1}{2\beta_{\omega_0}}\frac{\partial^2 w}{\partial x^2} + \frac{\chi^{(2)}\omega_0}{2\,\mathrm{cn}_{\omega_0}}\frac{\int V|W|^2 \mathrm{d}y}{\int |W|^2\,\mathrm{d}y} vw^* \exp(-j\Delta kz) = 0,$$

$$j\frac{\partial v}{\partial z} - j\beta_{2\omega_0}{}'\frac{\partial v}{\partial t} - \frac{\beta_{2\omega_0}{}''}{2}\frac{\partial^2 v}{\partial t^2} + \frac{1}{2\beta_{2\omega_0}}\frac{\partial^2 v}{\partial x^2} + \frac{\chi^{(2)}\omega_0}{2\,\mathrm{cn}_{2\omega_0}}\frac{\int V|W|^2 \mathrm{d}y}{\int |V|^2\,\mathrm{d}y} w^2 \exp(j\Delta kz) = 0, \quad (1)$$

where β represents the propagation constant, β' is the inverse group velocity, and β'' is the inverse group-velocity dispersion; n is the refractive index, $\Delta k = 2\beta_{\omega_0} - \beta_{2\omega_0} + K_S$, where $K_S = 2\pi/\Lambda$ and $\chi^{(2)} = 2/\pi\chi^{(2)}_{z'z'z'}$ is the nonlinear coefficient.

We employed a finite-difference vectorial mode solver to determine the linear propagation properties in the slab waveguide, i.e., the mode profiles, $\beta_{\omega_0}, \beta_{2\omega_0}, \beta_{\omega_0}{}', \beta_{2\omega_0}{}', \beta_{\omega_0}{}''$, and $\beta_{2\omega_0}{}''$. Under these conditions the crystal length corresponds to 3.2 times the FF diffraction length and to 4.8 times the walk-off length between the FF and the SH. Finally, using a finite-difference beam propagation technique, we solved the nonlinear coupled equations [Eqs. (1)].

We carried out experiments and numerical simulations, varying the phase-mismatch conditions by changing the temperature of the sample or the input pulse power, keeping fixed the temporal and spatial widths of the FF injected pulse.

First we measured the spatial profiles of the FF output beam along the free propagation direction relative to the injected power at different phase mismatches. We compared measured normalized output profiles in the quasi-linear and nonlinear trapped regimes at a fixed phase mismatch. Typical experimental results (dotted curves) and numerical results (solid curves) are shown in Fig. 1 (top). In the quasi-linear regime the output beam profile had a width $w_{0x} = 246\ \mu$m that corresponds to the diffracted input beam ($w_{0x} = 76\ \mu$m) after 58 mm of propagation along the waveguide. Increasing the incident intensity causes the nonlinear self-focusing to balance the effect of diffraction. Figure 1 (bottom) illustrates the typical dependence of the output spatial profile's width on the injected intensity at a fixed phase mismatch (the solid curve refers to numerical results; filled circles, to experimental data). In the limit of the available power (590 W) it was not possible to observe self-trapping in the close vicinity of perfect phase matching ($\Delta kL = 0$), which was measured to occur at $T = 160$ °C. Spatial trapping started to appear at a sample temperature of 151°C ($\Delta kL \sim 9\pi$) and was maintained (with a linear increase in the power threshold) to $T = 114$ °C ($\Delta kL \sim 46\pi$); this trend is illustrated in Fig. 2. Figures 1 and 2 clearly demonstrate that self-trapped beams have been generated despite walk-off and short-pulse excitation. Thus group-velocity mismatch can prevent spatial trapping near phase matching, but trapping does occur at a large enough phase mismatch, in agreement with the prediction of Ref. 7.

The temporal behavior of these self-trapped beams has also been analyzed. Typical FF and SH pulse temporal envelopes, when nonlinear self-focusing balances the effect of diffraction, are shown in Fig. 3 (top). Despite a strong walk-off, the pulse at the FF and a consistent contribution at the SH overlap in time and lock together, thus providing an appreciable self-focusing effect by cascading. However, when the nonlinear effect does not balance the spatial diffraction, we note that the FF and the SH pulses do not overlap in time and do not lock together. This property was also been revealed experimentally during the measurement of cross-correlation traces. In the FF output pulse we notice a self-steepening of the trailing edge that is due to locking with the SH component. In Fig. 3 (bottom) we compare the intensities of the measured and

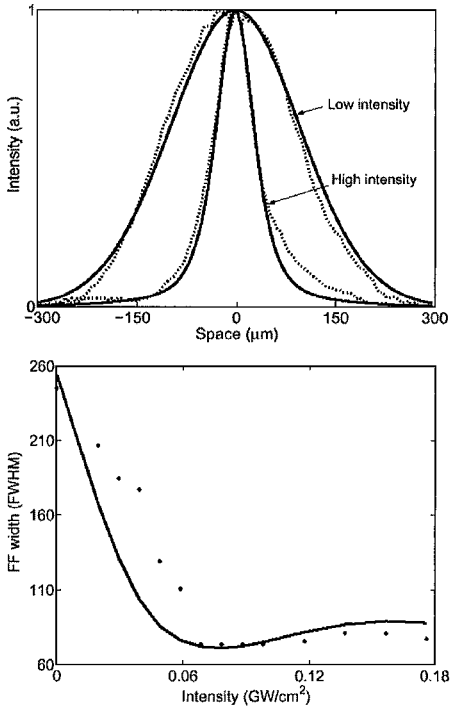

Fig. 1. Top, spatial profile of the FF output in the quasi-linear regime (low intensity) and in the self-trapped regime (high intensity, $I = 66$ MW/cm^2); dotted curves, experimental data; solid curves, numerical simulations. Bottom, evolution of the FF output beam's FWHM versus input FF intensity; filled circles, experimental data; solid curve, simulations. Here $\Delta kL = 18\pi$.

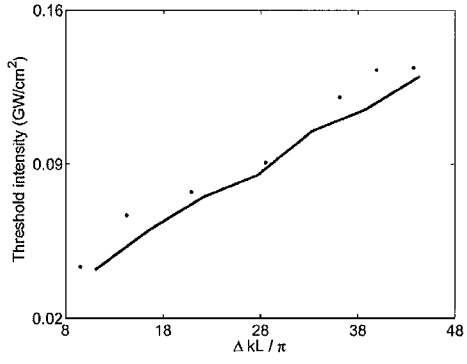

Fig. 2. Power threshold of self-trapping versus phase mismatch. Filled circles, experimental data; solid curve, numerical simulations.

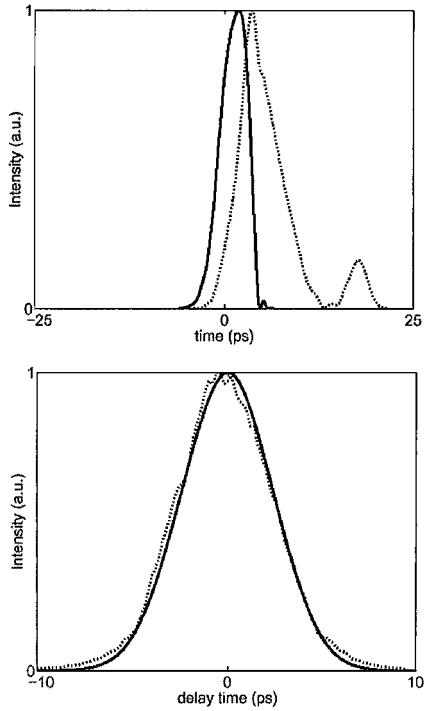

Fig. 3. Top, calculated FF (solid curve) and SH (dotted curve) pulses at output. Bottom, autocorrelation traces in intensity of the FF at output (solid curve, numerical simulation; dotted curve, experimental data). Here $\Delta kL = 18\pi$ and $I = 66$ MW/cm^2.

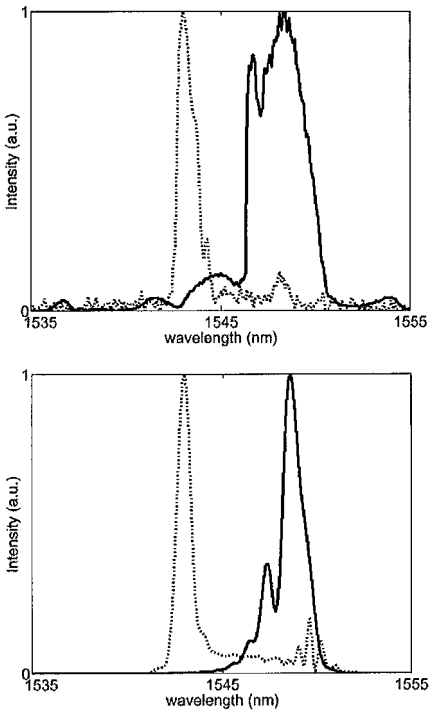

Fig. 4. Top, measured and bottom, calculated output pulse spectra at the FF (solid curves) and at the SH (dotted curves) after a twofold expansion of the SH scale. Here $\Delta kL = 18\pi$ and $I = 120$ MW/cm^2.

simulated autocorrelation traces of the FF at output. We stress that the autocorrelation process masks the pulse asymmetry and that the durations of the input and output pulses were approximately equal.

Clearly, the self-focusing effect may involve spectral distortions; contrary to what happened in the quasi-cw experiments,[5] strong spectral changes were expected because the input pulse's spectrum can be significantly broader than the SH-generated spectral acceptance of the sample. Moreover, at high input power, spectral broadening of the fundamental, which was due to self-phase modulation through cascading, was clearly observed. Consequently, because of intraspectral SH generation with different phase-matching conditions, the spectra of FF and SH are modified asymmetrically. Figure 4 shows typical spectral distortions of the FF and the SH after a twofold expansion of the SH coordinates. Note the FF spectral broadening together with a frequency shift of both the FF and SH peaks as a result of asymmetry of the phase-matching condition on the wide FF spectra. Both the spectral broadening and the frequency shift of the FF and SH peaks depend consistently on the injected FF intensity and on the phase-mismatch conditions.

In conclusion, we have proved the possibility of exciting spatially trapped beams in Ti-indiffused $LiNbO_3$ slab waveguides with few-picosecond pulses that are significantly shorter than the temporal walk-off between fundamental and second-harmonic waves, with only a FF ($\lambda = 1548$ nm) at the input. We carried out a numerical and experimental study to determine the influence of phase mismatch and of pulse power on the trapping effect. The temporal and spectral properties that accompany self-trapped propagation have been described.

This study was performed in the frame-work of the European project ROSA (Information Society Technologies Programme/Future & Emerging Technologies) supported by the European Commission. The authors thank L. Torner and S. Carrasco for fruitful discussions and comparison of our results with simulations. A. Barthelemy's e-mail address is abarth@ircom.unilim.fr. F. Baronio is also with the Istituto Nazionale per la Fisica della Materia, Università di Padova, Via Gradenigo 6/a, 35131 Padua, Italy.

References

1. G. I. Stegeman, D. J. Hagan, and L. Torner, Opt. Quantum Electron. **28,** 1691 (1996).
2. Y. N. Karamzin and A. P. Sukhorukov, Sov. Phys. JETP **41,** 414 (1976).
3. M. J. Werner and P. D. Drummond, Opt. Lett. **19,** 613 (1993).
4. W. E. Torruellas, Z. Wang, D. J. Hagan, E. W. Van Stryland, G. I. Stegeman, L. Torner, and C. R. Menyuk, Phys. Rev. Lett. **74,** 5036 (1995).
5. R. Schiek, Y. Baek, G. Krijnen, G. I. Stegeman, I. Baumann, and W. Sohler, Opt. Lett. **21,** 940 (1996).
6. S. Kim, Z. Wang, D. J. Hagan, E. W. Van Stryland, A. Kobyakov, F. Lederer, and G. Assanto, IEEE J. Quantum Electron. **34,** 666 (1998).
7. S. Carrasco, J. P. Torres, D. Antigas, and L. Torner, Opt. Commun. **192,** 347 (2001).